water

MDPI

Article

Removal of Contaminants of Emerging Concern from Wastewater Using an Integrated Column System Containing Zero Valent Iron Nanoparticles

Evridiki Barka, Constantinos Noutsopoulos *, Andriani Galani, Iliana Panagou, Maria Kalli, Elena Koumaki, Simos Malamis and Daniel Mamais

Sanitary Engineering Laboratory, Department of Water Resources and Environmental Engineering, School of Civil Engineering, National Technical University of Athens, 15780 Athens, Greece
* Correspondence: cnoutso@central.ntua.gr

Abstract: Non-steroidal anti-inflammatory drugs (NSAIDs) and endocrine disruptors (EDCs) are among the most important categories of contaminants of emerging concern (CECs), and many advanced technologies have been developed for their elimination from water and wastewater, including nano-zero valent iron (nZVI). This study investigates the performance of nZVI synthesized from green tea extracts and incorporated into a cationic resin (R-nFe) in the removal of four selected NSAIDs, namely ibuprofen (IBU), naproxen (NPX), diclofenac (DCF), and ketoprofen (KFN), and an EDC, namely bisphenol A (BPA). Column experiments were conducted to evaluate the effect of various operating parameters, including initial CECs concentration, contact time, pH, addition, and dose of sodium persulfate (PS). To the authors' knowledge, this is the first time that environmentally friendly produced nZVI has been combined with PS in column experiments for the removal of CECs from wastewater. With a contact time of 2.2 min, PS = 1 mM, and influent pH = 3.5, 27–72% of IBU, 70–99% of NPX, 70–95% of DCF, 28–50% of KFN, and 61–91% of BPA were removed during a 12-day operation of the system, while the initial concentration of each substance was 5 μg/L. Therefore, it is anticipated that the proposed system could be a promising post-treatment technology for the removal of CECs from wastewater.

Keywords: emerging contaminants; non-steroidal anti-inflammatory drugs; endocrine disruptors; nano zero valent iron; advanced oxidation processes

Citation: Barka, E.; Noutsopoulos, C.; Galani, A.; Panagou, I.; Kalli, M.; Koumaki, E.; Malamis, S.; Mamais, D. Removal of Contaminants of Emerging Concern from Wastewater Using an Integrated Column System Containing Zero Valent Iron Nanoparticles. *Water* **2023**, *15*, 598. https://doi.org/10.3390/w15030598

Academic Editor: Alexandre T. Paulino

Received: 14 December 2022
Revised: 28 January 2023
Accepted: 31 January 2023
Published: 3 February 2023

1. Introduction

In recent decades the occurrence of micropollutants in the surface and groundwater has become an issue of great concern worldwide. Micropollutants or emerging pollutants (EPs), also known as emerging contaminants or contaminants of emerging concern (CECs), are synthetic or natural compounds that enter the environment and can have adverse effects on humans and ecosystems [1], also posing a threat to the sustainability of freshwater resources. They include a wide range of substances, such as pharmaceuticals and personal care products, agrochemicals, such as pesticides and herbicides, and other industrial chemicals, such as plasticizers, flame retardants, food additives, etc. [2]. Although they are found in trace concentrations (ng/L to μg/L) [3,4] in water bodies and wastewater, their continuous discharge and stability lead to bio-accumulation in ecosystems and living organisms and biomagnification in some species through the trophic chain [5], increasing awareness of their potential toxicity. Furthermore, synthetic chemicals can be transformed into intermediate products with different physicochemical properties and ecotoxicological profiles, depending on the environment in which they occur (e.g., groundwater, surface water, sediments, wastewater treatment plants, drinking water facilities) [6]. Endocrine disrupting chemicals or endocrine disruptors (EDCs) and non-steroidal anti-inflammatory drugs (NSAIDs) are two main subgroups of CECs, while according to researchers [7,8]

some NSAIDs (such as ibuprofen, diclofenac, and naproxen) can also cause endocrine disruption. As Gao et al. [9] has reported, EDCs can be harmful to humans, as they can impair reproductive and developmental functions, reduce human immunity, induce tumors, and cause neurological disorders, while remasculinization and feminization [10–12], metabolic disorders [13], and adverse effects on reproduction and development [14–17], and on the immune and nervous systems [16–18], have been reported in wildlife. The NSAIDs are a very important subcategory of pharmaceuticals as they are consumed in large quantities each year, are found worldwide, and are bioactive and potentially toxic when present in aquatic environment [19]. According to Świacka et al. [8], NSAIDs can negatively affect non-target aquatic animals on many levels, both in terms of behavior and physiology, and in the form of genetic changes or reproductive disorders that affect the development of entire populations.

Wastewater from households, industry, and hospitals is the main sources of EDCs in wastewater treatment plants (WWTPs) [20], while NSAIDs enter the sewerage system mainly due to incomplete metabolization in humans and their consecutive excretion in urine and feces, as well as due to incomplete metabolization in animals, accounting for up to 15% of all pharmaceuticals detected in water bodies globally, either as unchanged drugs or as parent/metabolized compounds [19]. As conventional wastewater treatment processes are unable to efficiently eliminate these recalcitrant compounds [9], they are continuously released into the aquatic environment. In the effluent stream of WWTPs, concentrations of NSAIDs are typically up to μg/L [21], while concentrations of EDCs range between sub-ng/L and μg/L [20]. Several advanced technologies have been developed to remove EDCs and NSAIDs from water and wastewater matrices. These technologies include adsorption on materials, such as organoclay [22,23], ordered mesoporous carbon and activated carbon [24–26], and various advanced oxidation processes (AOPs).

Advanced oxidation processes (AOPs) have been proposed as a method that promotes the degradation of CECs through a high-efficient and environmentally compatible technology, since no secondary pollution is expected [27]. These AOPs are generally based on the formation of hydroxyl radicals (HO), which are non-selective oxidants for organic compounds. In recent years, sulfate radicals (SO_4^{-}) have gained interest, since they exhibit higher selectivity and, in some cases, better degradation efficiencies [28], which can be attributed to higher redox potential (E_0 = 2.5–3.1 V) compared to hydroxyl radicals (E_0 = 1.8–2.7 V) [29]. Moreover, sulfate radicals have a longer half-life and higher reactivity over a wide pH range (3–7) [29].

Furthermore, AOPs include a wide variety of technologies, such as ozone [30–32], photocatalysis [33–37], UV/H_2O_2 [38,39], homogeneous or heterogeneous Fenton reaction processes [40], sonolysis [41,42] activation of persulfate (PS), and peroxymonosulfate (PMS) by various methods, such as thermal, alkaline, UV light, activated carbon, transition metal, ultrasound, etc., [28,43] and, recently, the activation of peracetic acid by different techniques, including ferric ions [44] or microwaves [45]. However, the widespread use of AOPs is still limited due to high costs and demanding reaction conditions [27].

Research into cost-effective and environmentally friendly methods for treating CECs is still ongoing. Nanotechnology, and in particular nano zero valent iron (nZVI), has recently attracted interest in the remediation of organic micropollutants, as it has been proved to be a very efficient technology for the treatment of many pollutants, such as TCE [46,47], organic dyes [48,49], heavy metals [50–52], pesticides [53–55], PAHs [56], etc. Nanoparticles (NPs) can be synthesized through physical and chemical methods, such as mechanical milling, electrospinning, lithography, sputtering, chemical vapor deposition, solvothermal and hydrothermal methods, the sol–gel method, and chemical reduction [57–59]. Some of the main disadvantages of these methods are the high costs, the long processing times, the use of toxic reducing agents, and the irregular shape of the NPs. Nowadays, green synthesis methods using environmentally friendly materials and techniques for the production of NPs are being promoted, such as plant extracts as reducing agents that replace the toxic chemical sodium borohydride ($NaBH_4$). Although nZVI has been used in column

experiments and pilot scale applications for the in situ remediation of TCE [60], heavy metals [61–66], PCE [67], PAHs [68], explosive materials [69], and dyes [70,71], most of the experiments on the treatment of CECs are related to batch testing, and research is very sparse [72,73], with continuous flow experiments simulating real conditions.

This study aims to fill this gap by using nZVI in column systems to evaluate the removal efficiency of selected NSAIDs and EDCs from wastewater, with and without the addition of an oxidative reagent that involves AOPs. To achieve this goal, nano zero valent iron was incorporated into a cationic resin through an environmentally friendly synthesis method where the adsorbed trivalent iron is reduced to zero valent though the application of polyphenols produced by green tea extract. The resin not only serves as a carrier material for the nZVI to ensure that the nanoparticles do not escape together with the treated medium, but also as a suitable sorbing medium for column systems. Other researchers have used biopolymers, such as alginate beads, to cage NPs [74]. In addition, the resin does not allow the agglomeration of the nanoparticles, and the polyphenols act both as a reducing and capping agent, prolonging the reactivity of the nZVI. The synthesized nanocomposite was named R-nFe. To the authors' best knowledge, this is the first study where green tea-produced nZVI is used in combination with an oxidative reagent in column experiments to treat CECs from wastewater. The target compounds of the present study were ibuprofen (IBU), naproxen (NPX), diclofenac (DCF), and ketoprofen (KFN) for the NSAIDs category, and bisphenol A (BPA) for the EDCs group. Here, BPA is a synthetic estrogen used to harden polycarbonate plastics and epoxy resins [75], whereas IBU, NPX, DCF, and KTP are pharmaceutical compounds commonly used to relieve pain and inflammations. The DCF and IBU compounds are the most frequently detected NSAIDs globally, with NPX and KFN following [76]. The main objectives of the present study were the investigation of the effects of different parameters, such as contact time, initial concentration of target compounds, influent pH, synergy and dose of an oxidative reagent, and the development of an integrated treatment system. During the experimental period, two (2) potential oxidative reagents were tested in batch experiments as potential candidates to be combined with the nanocomposite material, namely sodium persulfate (PS) and hydrogen peroxide (H_2O_2).

2. Materials and Methods

2.1. Materials

The resin, Amberlyst 15 hydrogen form (H^+) wet, was purchased from Sigma-Aldrich (Steinheim, Germany), and a commercial green tea product (Twinings of London, Swarzedz, Polland) was used for the production of the extract. Sodium chloride (NaCl) and iron chloride hexahydrate ($FeCl_3 \cdot 6H_2O$) was purchased from Honeywell Fluka (Seelze, Hannover, Germany). Folded filters (4–12 μm) and membranes with a pore size of 0.45 μm were both purchased from Whatman (Dassel, Germany). High purity grade standards, namely BPA (≥99.0%), IBU (≥99.8%), NPX (≥98.0%), DCF (≥99.7%), KFN (≥98.0%), deuterated bisphenol A (BPA-d16) (≥99.0%), and meclofenamic acid sodium salt (MCF) (≥93.0%) were obtained from Sigma-Aldrich (Steinheim, Germany). Stock solutions of high concentrations (1000 ppm) were prepared for each compound and kept at −18 °C. Methanol (MeOH) and ethyl acetate (ETH) of high-performance liquid chromatography (HPLC) grade were purchased from Merck (Darmstadt, Germany) and Honeywell (Seelze, Hannover, Germany), respectively. Isolute cartridges of C18 500 mg/6 mL, used for solid phase extraction (SPE), were purchased from Biotage (Uppsala, Sweden). Pyridine and bis(trimethylsilyl)trifluoroacetamide (BSTFA) +1% trimethylchlorosilane (TMCS), used for silylation, were purchased from Sigma-Aldrich (Steinheim, Germany). Ultra-pure HCl (32%), used for acidification of the samples and pH adjustment, was purchased from Sigma-Aldrich (Steinheim, Germany). Hydrogen peroxide (H_2O_2) solution (30% w/w) and sodium persulfate ($Na_2S_2O_8$) of a high purity grade (>98%) were purchased from Honeywell, Fluka (Seelze, Hannover, Germany), and Sigma-Aldrich (Steinheim, Germany), respectively. Ultrapure water was prepared in the laboratory with the use of a Milli-Q/Milli-RO Millipore system (Millipore, Billerica, MA, USA).

2.2. R-nFe Synthesis

The R-nFe composite material was synthesized following the method proposed by Toli et al. [52], and a pretreatment step using 1 M NaCl solution was also performed, since it has a positive effect on the removal efficiency of the pollutants, as recently proposed by Panagou et al. [77]. The synthesis procedure consisted of the following steps: (1) the cationic resin Amberlyst 15 H^+ in its wet form was agitated at 200 rpm for 2 h with NaCl solution (1 M) in order to reduce the acidity. The resin that was produced mainly carries on Na^+ ions and is called R-Na. (2) R-Na was agitated with $FeCl_3$ $6H_2O$ solution 0.05 M at 200 rpm for 4 h. Here, Fe^{3+} replaced Na^+ ions due to the higher electrostatic affinity from the sulfonic groups of the resin. The resin with the adsorbed Fe^{3+} species is called R-Fe. (3) The R-Fe was agitated with green tea extract for 20 h with the aim of reducing the Fe^{3+} species to Fe^0 by polyphenols, generating the final composite material that is called R-nFe. Finally, (4) the R-nFe was treated with 1 M NaCl solution with a mixing ratio of 100 g R-nFe/1000 mL NaCl solution as a pre-treatment step that was performed 1 day before the use of the R-nFe in each experiment. The same nanocomposite material has been used in a previous study, and information about the morphology of the resin beads and elemental analysis of the observed surfaces is provided there in detail [77]. The SEM analysis indicated that iron content was uniformly distributed, while the TEM analysis showed that iron nanoparticles had a spherical shape and size in the order of 20–40 nm. An EDS analysis was also performed in the same study.

2.3. Wastewater Source and Characteristics

All column experiments were performed using tertiary treated wastewater from the main wastewater treatment plant of Athens (Psyttaleia). The main quality parameters of the wastewater are summarized in Table 1.

Table 1. Wastewater characteristics used in the experiments.

Parameter	Tertiary Effluent (Average ± Stdev)	Units
pH	7.30 ± 0.1	
Alkalinity	160 ± 23	mg $CaCO_3$/L
Electric conductivity	1354 ± 50	μS/cm
Total organic carbon (TOC)	12 ± 3	mg/L
Total chemical oxygen demand (CODt)	32.4 ± 1.20	mg/L
Total suspended solids (TSS)	0.64 ± 0.17	mg/L
Nitrate	7.13 ± 0.11	mg/L
Sulfate anions	94 ± 11	mg/L
Bisphenol-A (BPA)	192 ± 51	ng/L
Ibuprofen (IBU)	<LOQ [1]	ng/L
Naproxen (NPX)	155 ± 4	ng/L
Diclofenac (DCF)	585 ± 60	ng/L
Ketoprofen (KTP)	457 ± 50	ng/L

[1] <limit of quantification = 30 ng/L.

2.4. Experimental Set-Up

Within the context of this experimental work, two types of experiments were conducted—batch tests and continuous flow experiments (column experiments)—in order

to study the effect of different parameters on the removal of selected CECs with a combination of nanotechnology (nZVI) and advanced oxidation processes (AOPs). The target compounds of the present study were ibuprofen (IBU), naproxen (NPX), diclofenac (DCF), ketoprofen (KFN), and bisphenol A (BPA).

2.4.1. Batch Experiments

The goal of the batch experiments was the selection of the most suitable oxidative reagent for combination with R-nFe material. The synergistic effect of two oxidative reagents, sodium persulfate (PS) and hydrogen peroxide (H_2O_2), with the R-nFe material was investigated. The matrix used was distilled water. The initial concentration of the compounds was 10 μg/L, while the R-nFe concentration was 15 g/L. The pH was adjusted to an acidic value of 3–3.5. Schott glass bottles of 1 L each were used. Three different concentrations (1, 2, and 3 mM) were tested at two different contact times (30 and 60 min) at a stirring speed of 200 rpm. In addition, the combination of 1 mM PS with 1 mM H_2O_2, in the presence of R-nFe, was performed to investigate whether the cheaper H_2O_2 can partially replace PS. Control experiments were also performed using only PS or only H_2O_2 at three different concentrations (1, 2, and 3 mM) and only R-nFe at 15 g/L. In Table 2, a detailed description of the experimental conditions in every batch experiment is provided.

Table 2. Experimental conditions studied in the batch tests.

Experimental Conditions	Batch Test Name	CECs	R-nFe	PS	H_2O_2	pH
		μg/L	g/L	mM	mM	
Effect of R-nFe	R-nFe	10	15	-	-	3–3.5
Effect of H_2O_2	H_2O_2 1mM	10	-	-	1	3–3.5
	H_2O_2 2mM		-	-	2	
	H_2O_2 3mM		-	-	3	
	R-nFe + H_2O_2 1mM		15	-	1	
	R-nFe + H_2O_2 2mM		15	-	2	
	R-nFe + H_2O_2 3mM		15	-	3	
Effect of PS	PS 1mM	10	-	1	-	3–3.5
	PS 2mM		-	2	-	
	PS 3mM		-	3	-	
	R-nFe + PS 1mM		15	1	-	
	R-nFe + PS 2mM		15	2	-	
	R-nFe + PS 3mM		15	3	-	
Effect of R-nFe, H_2O_2, and PS	R-nFe + H_2O_2 1mM + PS 1mM	10	15	1	1	3–3.5

2.4.2. Column Experiments

In the continuous flow study, experiments were carried out using four columns made of cell cast acrylic material (plexiglass), with a height of 1.40 m and a circular cross-section with an inner diameter of 0.05 m, in different configurations. Each column was filled with R-nFe and, to prevent material loss, a 1 cm layer of glass wool was placed at the bottom. The plastic tank feeding the system contained tertiary effluent, and target pollutants were added at the desirable concentration. Continuous downward flow was applied using a peristaltic pump, at a constant flowrate of approximately 26 L/day. Each column was equipped with a sampling port located at the bottom of each column.

The column experiments were conducted in two phases. In the first phase, the experiments were conducted with four columns connected in series in order to investigate the effect of contact time and initial concentration of the target compounds. The contact times

tested were 2.2, 4.4, 6.6, and 8.8 min, while the initial concentrations of CECs were 1 and 5 µg/L. These values were chosen according to the range of the concentration of emerging contaminants in the treated wastewater that mostly varies from a few ng to a few µg per liter [5,19,78,79]. The general configuration is shown in Figure 1a. Practically, this set-up enabled the simulation of four different bed heights, with the bed height of the last column being four times taller (40 cm) than the first column's bed height (10 cm).

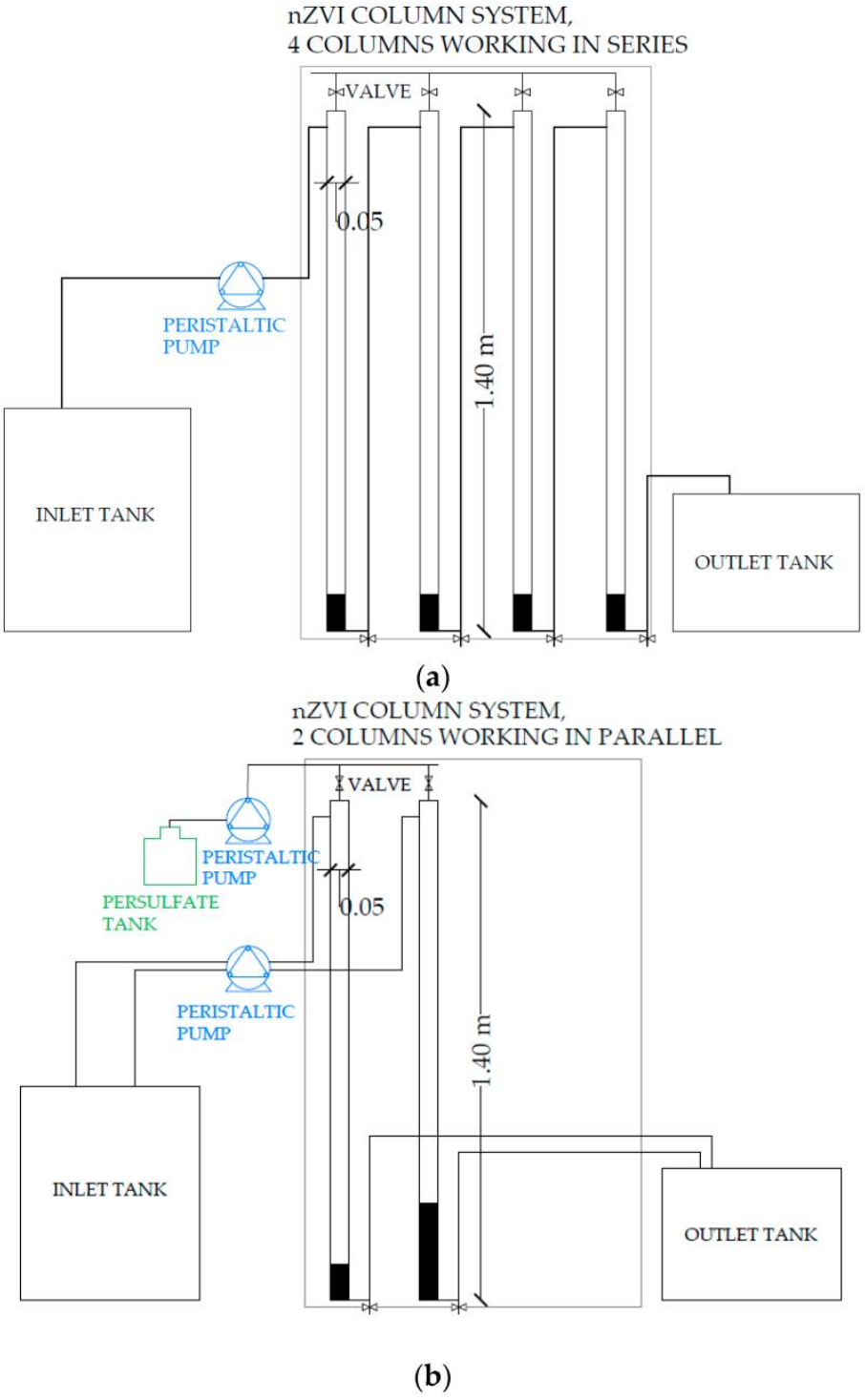

Figure 1. The general configuration of the nZVI column system working in series (**a**) and working in parallel (**b**).

In the second phase, the column experiments were continued with the two columns of the original system working in parallel, while the initial concentration of the compounds was 5 μg/L. In this phase, the effects of pH adjustment on the influent matrix and contact time at a controlled pH were investigated by performing an experiment with pH adjustment to acidic values for two alternative contact times (2.2 and 4.4 min). Furthermore, column experiments were performed at acidic pH with PS addition which, according to the batch experiments, was the optimum oxidative reagent. The PS was supplied to the columns with a peristaltic pump (Shenchen LabM6, Baoding Shenchen Precision Pump Co., Ltd., Baoding, China). The flow rate of the PS solution was 1.2 L/d. The general configuration is shown in Figure 1b. The effect of PS dose was investigated by performing two experiments at a contact time (CT) of 2.2 min with concentrations of 1 and 5 mM, chosen in accordance with the concentration range of PS used in the batch experiments and in other studies [29,75,80–83].

All experiments (column and batch) took place under aerobic conditions (DO = 6–8 mg/L), and the temperature ranged from 17–26 °C. The main parameters of each experimental run of the column system are summarized in Table 3.

Table 3. Experimental conditions studied in the column experiments.

Column Experiment	CECs	Contact Time	PS	pH
	μg/L	Minutes	mM	
Effect of CECs' initial concentration	1 and 5	8.8	-	7
Effect of contact time	5	2.2, 4.4, 6.6, and 8.8	-	7
Effect of pH adjustment and contact time	5	2.2 and 4.4	-	3.5 and 7
Effect of oxidative reagent dose	5	2.2	1 and 5	3.5

2.5. Elaboration of Data

Contact time was calculated using the following Equation (1):

$$CT = \frac{\theta \times A \times H}{Q} \quad (1)$$

while θ (the external porosity) was given by the following Equation (2):

$$\theta = 1 - \frac{\rho_{bulk}}{\rho_{particle}} \quad (2)$$

where ρ_{bulk} is the bulk density, which is equal to the following:

$$\rho_{bulk} = \frac{A \times H}{M} \quad (3)$$

where A is the surface area of the cross-section equal to 20 cm^2, H is the height of the filling material, M is the mass of the R-nFe material, $\rho_{particle}$ is the particle density equal to 1278 kg/m^3, and Q is the flowrate equal to 26 L/d.

2.6. Sampling Procedure

Sampling was performed at predetermined time intervals. In the column experiments, liquid samples were collected from the sampling port at the bottom of each column, while in the batch tests, samples were withdrawn from the Schott bottles. Collected samples were then filtered through 0.45 μm membranes, acidified with 2 N HCl to a pH of 2.5, and stored at 4 °C for a maximum of 48 h before analysis.

2.7. Analytical Methods

The qualification and quantification of the target compounds (IBU, NPX, DCF, KFN, and BPA) was carried out according to the analytical method developed by Samaras et al., 2011 [84]. The main steps of this method are as follows: (i) filtration of the samples, (ii) acidification (pH = 2.5), (iii) addition of the surrogates, (iv) solid phase extraction where elutions of 6 mL of ETH are produced, (v) evaporation of the elusions to dryness under nitrogen purge (N_2), (vi) derivatization with 10 μL pyridine and 50 μL BSTFA + 1% TMCS at a bathing device of 70 °C for 20 min, and, finally, (vii) GC–MS analysis. Here, BPA-d16 and MCF are used as surrogates for the EDC and NSAIDs, respectively. The gas chromatograph (GC) was a 7890A, and the mass selective detector (MSD) was a 5975C from Agilent Technologies. The software used was Agilent ChemStation.

3. Results and Discussion

3.1. Effect of Target Compounds Initial Concentration

The effect of the target compounds' initial concentration on CECs removal was investigated by conducting experiments at initial concentrations of 1 and 5 μg/L. Figure 2 shows the evolution of DCF and BPA during the operating time of the column system for the contact time of 8.8 min. The figures for the evolution of IBU, NPX, and KFN are provided in the Supplementary Materials (Figure S1). It is observed that with the increase in the initial concentration from 1 to 5 μg/L, the performance of the R-nFe column for the removal of IBU, NPX, DCF, and KFN declined. The ratio of the mass of the pollutant removed per mass of the nanocomposite material (R-nFe) at the end of each experiment (Table 4) increases for all the target compounds at the higher concentration (C_0 = 5 μg/L), especially in the case of BPA. The main possible removal mechanisms involved are adsorption into the surface of (hydro)oxides of nZVI or into the resin, oxidation by radicals through a Fenton-like mechanism with a small contribution depending also on the availability of H^+ ions and reduction for the case of DCF. The ability of the R-nFe to remove the target NSAIDs is reduced faster in the case of the 5 μg/L initial concentration, indicating an exhaustion of the active sites for adsorption and other mechanisms (oxidation, reduction) which occur to a lower extent. However, BPA molecules continued to be removed at the highest initial concentration, indicating no saturation until 192 h of operation, showing an enhanced process longevity and removal ability. Regarding other studies in the literature, Sulaiman and Al-Jabari [73] noticed a slight reduction in the removal of DCF when the initial concentration increased in their column tests using sand and nZVI supported on bentonite. It is emphasized that this is the second time that nZVI has been evaluated in column systems for the removal of CECs.

Table 4. The ratio of mass of pollutant removed per mass of the nanocomposite material (R-nFe) at the end of each experiment, conducted with two different initial concentrations of the pollutants (without pH adjustment and at a contact time of 8.8 min).

Target Compound	Mass of Pollutant Removed per Mass of R-nFe (μg/g) at the End of Each Experiment (CT = 8.8 min)	
	C_0 = 1 μg/L	C_0 = 5 μg/L
IBU	0.05	0.19
NPX	0.08	0.27
KFN	0.08	0.18
DCF	0.11	0.19
BPA	0.05	0.74

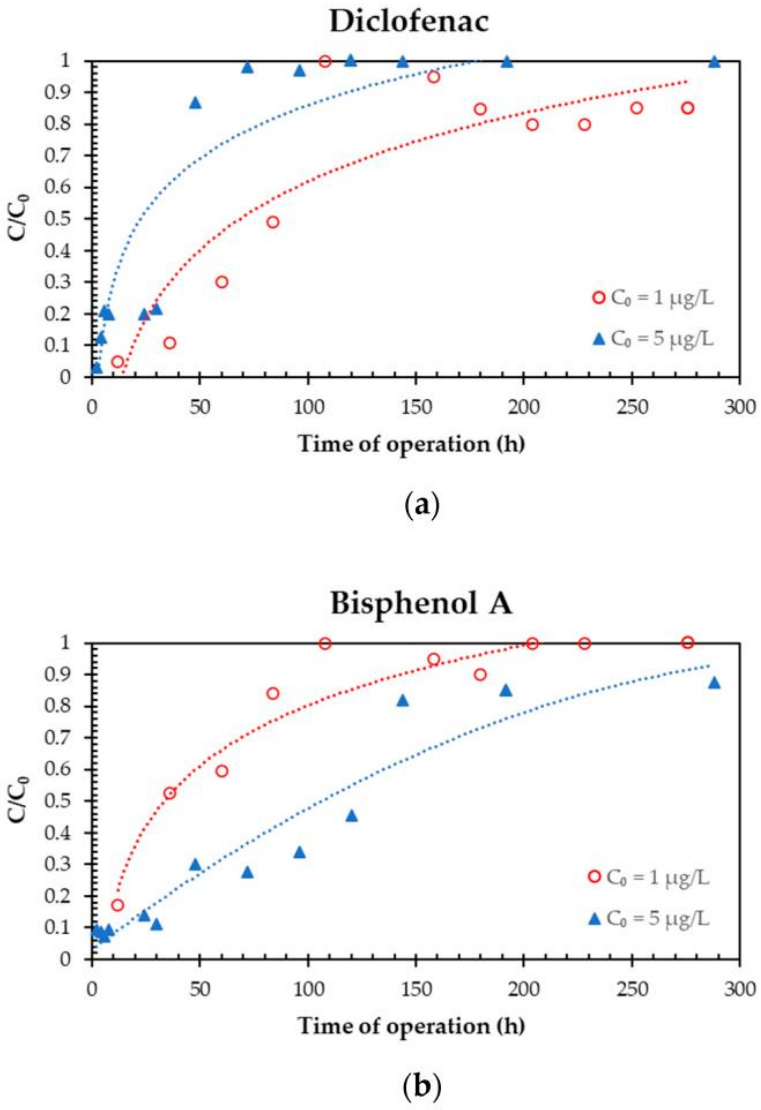

Figure 2. Effect of initial concentration on the removal efficiency of diclofenac (**a**) and bisphenol A (**b**) (Q = 26 L/d, CT = 8.8 min, no pH adjustment).

Panagou et al. [77] observed that with the increase in NSAID from 1 to 10 μg/L, R-nFe removal efficiency is significantly reduced at a dose of 15 g/L during batch experiments. Consistent with this finding, Ali et al. [85] observed during batch tests that the removal efficiency of amoxicillin by activated carbon from pomegranate peel coated with nZVI decreased with the increase in the concentration of amoxicillin due to the reduction in and saturation of active sites. Dehghani et al. [86] also found during batch tests that with the increase in the initial BPA concentration from 2 to 6 mg/L, removal efficiency of BPA using nZVI–chitosan slightly increased from 84% to 90%. They concluded that removal efficiency improved because more BPA molecules could be removed by the available surface area of nZVI–chitosan.

It seems that increasing the initial concentration of contaminants plays an important role in the longevity of the process. The performance of the system in terms of removal efficiency towards operating time declined for the IBU, NPX, DCF, and KFN when 5 μg/L was tested instead of 1 μg/L, while this was not the case for BPA. The initial concentration of 5 μg/L was adopted for the following experiments.

3.2. Effect of Contact Time

In this section, the effect of contact time is discussed, and the results for DCF and BPA are illustrated in Figure 3, while the graphs for the other compounds are shown in the Supplementary Materials (Figure S2). These experiments were conducted with no pH control. In order to investigate whether the effect of contact time was crucial for the performance of the column and whether lower contact times may facilitate similar removals, improving cost efficiency and treatment time, four different contact times were investigated with values between 2.2–8.8 min, at an initial CEC concentration of 5 μg/L. The decrease in contact time from 8.8 min to 2.2 min indicated a slight decrease in the removal efficiencies of NSAIDs achieved with R-nFe material; however, the ratio of pollutant mass removed per mass of nanocomposite material (R-nFe) did not significantly increase with the increase in contact time (Table 5). In general, all NSAID removal efficiencies were low for all CTs studied. More specifically, the concentration of IBU at the outlet of the R-nFe column with CT 2.2 min was approximately equal to that of the influent tank after 6 h of continuous operation, whereas for NPX, DCF, and KFN, this was observed at 24 h. Even with the longest contact time (CT = 8.8 min), the R-nFe column seemed insufficient to remove the selected NSAIDs after a period of 3 days of continuous operation. On the other hand, the effect of CT was more profound in the case of BPA. The performance of the R-nFe column was significantly better for BPA removal, with a removal efficiency of 90% after 2 h of continuous operation and approximately 10% after 72 h with contact time of 2.2 min. As shown in Table 5, the mass ratio of BPA removed per mass of R-nFe material remained almost constant for all CT studied. This enhanced performance was also evident in the case of the highest contact time studied (CT = 8.8 min), as the R-nFe material could no longer remove BPA after 192 h of continuous operation.

Table 5. The ratio of mass of pollutant removed per mass of the nanocomposite material (R-nFe) at the end of each experiment, conducted at four different contact times (initial concentration of each pollutant 5 μg/L, without pH adjustment).

Target Compound	Mass of Pollutant Removed per Mass of R-nFe (μg/g) at the End of Each Experiment (C_0 = 5 μg/L)			
	CT = 2.2 min	CT = 4.4 min	CT = 6.6 min	CT = 8.8 min
IBU	0.90	0.24	0.29	0.19
NPX	0.49	0.51	0.34	0.27
KFN	0.27	0.28	0.39	0.18
DCF	0.18	0.18	0.18	0.19
BPA	0.89	0.89	0.74	0.74

As mentioned above, these experiments were conducted with no pH control. A progressive increase in the pH value was observed in all columns, starting from acidic values (approximately 2.1–4.9) until it progressively reached the neutral pH of the inlet tank. Interestingly, the removal efficiencies in the case of the target compounds belonging to NSAIDs decreased gradually and concurrently with the increase in the pH value to alkaline levels. Therefore, it is anticipated that the role of pH may be more profound than the role of contact time for NSAID removal for the range of CTs studied. On the other hand, in the case of BPA, the removal efficiency remained high, even when the effluent pH was increased at values similar to the ones of the influent pH. This result was consistent for all the different contact times investigated. Thus, in the case of BPA, the effect of contact time is considered to be more significant than the effect of pH, showing that adsorption plays an important role in BPA removal. This could be attributed to the fact that pKa values of all selected NSAIDs vary from 4.14–4.59, whereas the pKa value of BPA is significantly higher (9.6). Thus, while the molecules of NSAIDs are changing their form from neutral to anionic [87], the form of BPA remained neutral in the pH range from 2.1–7.4 [88]. Furthermore, the nZVI

surface charge is considered to be neutralized at pH values around 7, while for lower pH values, the nZVI surface charge is positively charged [73,89]. In addition to pH, which as shown affects the extend of electrostatic interactions and adsorption of the compounds to the R-nFe material, dissolved oxygen may also exert an effect on CEC removal. It should be underlined that all columns were operated under aerobic conditions and, thus, dissolved oxygen may have triggered iron corrosion, resulting in higher concentrations of Fe^{+2} and Fe^{+3} ions in the liquid, thus, promoting the occurrence of Fenton reactions, as reported by other researchers [89,90]. In order to further study the effect of pH on CEC removal by the R-nFe columns, an additional experiment was conducted at controlled pHs, as described in the next section.

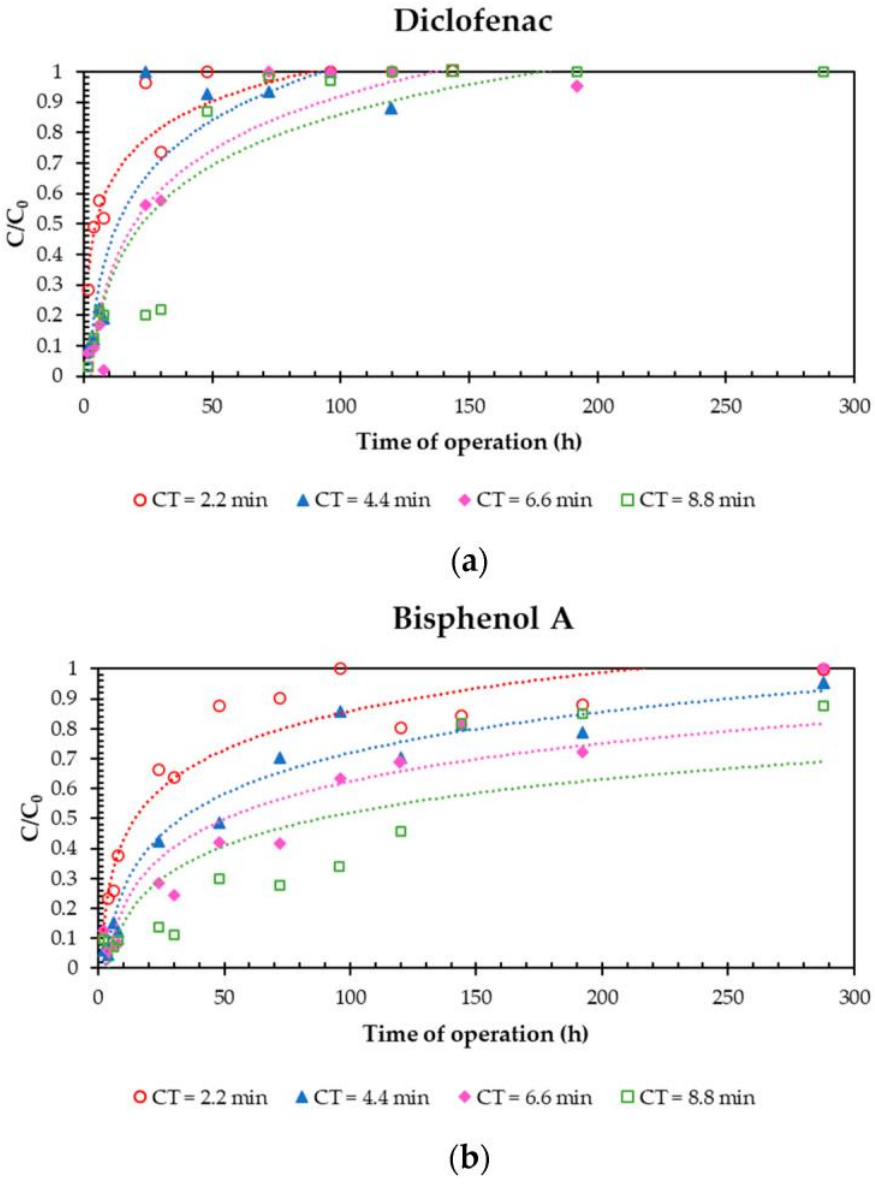

Figure 3. Effect of contact time on the removal efficiency of diclofenac (**a**) and bisphenol A (**b**) (Q = 26 L/d, C_0 = 5 μg/L, no pH adjustment).

3.3. Effect of pH Adjustment and Contact Time

The effect of pH on CEC removal was further investigated by conducting column experiments at lower CT values (2.2 min and 4.4 min). The acidic influent pH favored the removal efficiency of the target compounds, as illustrated in Figure 4 for DCF and BPA, and in the Supplementary Materials (Figure S3) for the other target compounds. The removal efficiencies for controlled and uncontrolled pH are displayed for the two

alternative contact times. One possible mechanism attributed to this pH effect could be the activation of the Fenton mechanism. At acidic pH, hydroxyl radicals can be formed according to Equations (4) and (5), where hydrogen peroxide can be generated from nZVI reacting with oxygen. Indeed, Fe^{2+} can be formed by the oxidation of nZVI through Equation (4), but also through Equations (6)–(8).

$$Fe^0 + O_2 + 2H^+ \rightarrow Fe^{2+} + H_2O_2 \quad (4)$$

$$Fe^{2+} + H_2O_2 \rightarrow Fe^{3+} + HO + OH^-, \text{ acidic pH} \quad (5)$$

$$Fe^0 + 2H^+ \rightarrow Fe^{2+} + H_2 \quad (6)$$

$$Fe^0 + H_2O + 0.5O_2 \rightarrow Fe^{2+} + 2OH^- \quad (7)$$

$$Fe^0 + 2H_2O \rightarrow Fe^{2+} + H_2 + 2OH^- \quad (8)$$

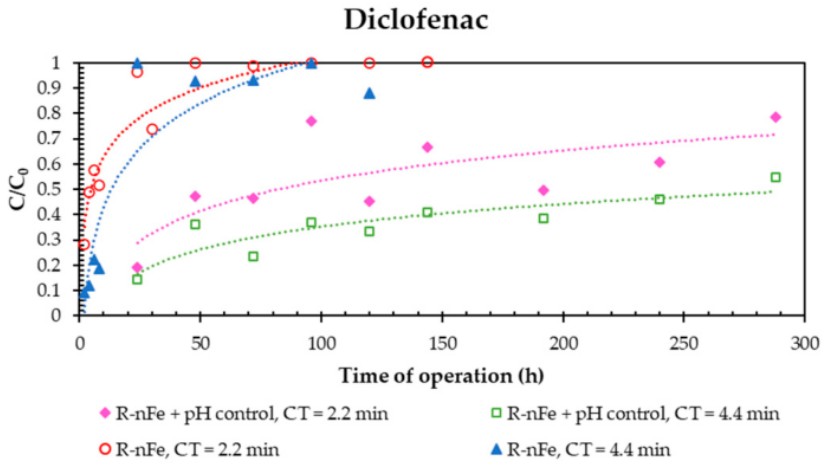

(**a**)

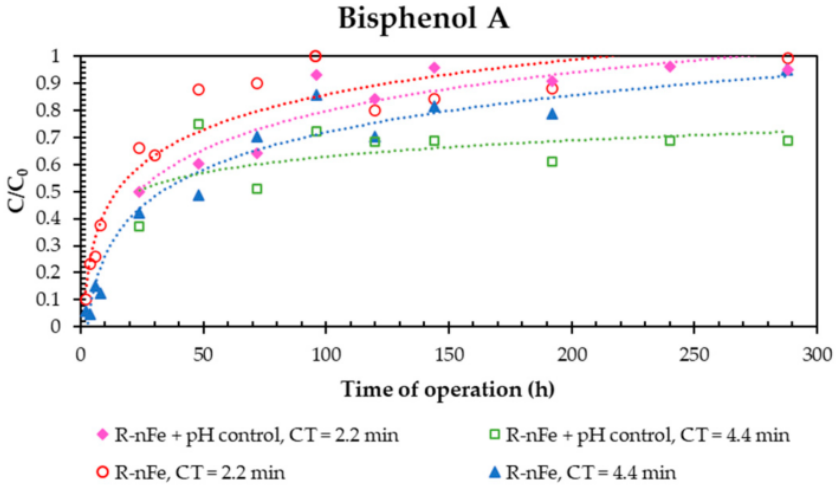

(**b**)

Figure 4. Effect of pH adjustment of the influent matrix to acidic values (approximately 3.5) and effect of contact time under acidic conditions on the removal efficiency of diclofenac (**a**) and bisphenol A (**b**) (Q = 26 L/d, C_0 = 5 μg/L).

In addition, acidic pH favors nZVI corrosion and dissolution of the passive film that gradually forms around the nanoparticles of zero valent iron, leading to the formation of more Fe^{2+} ions, which are used via the Fenton mechanism to create HO radicals [29,82,91].

In addition, the formation of iron oxides and hydroxides is promoted under neutral and alkaline conditions, leading to the passivation of nZVI and, thus, preventing iron corrosion and contact with pollutants [92]. Despite the positive effect of pH adjustment to obtain acidic values, the removal efficiency remains low to moderate after 2 days of operation, suggesting that an oxidative reagent may be required. The positive effect of pH adjustment to obtain acidic values, especially at pH 3, for the removal of NSAIDs and EDCs by nZVI, was also observed in our previous work in batch experiments [77]. Furthermore it is consistent with results of batch experiments reported by other researchers in the literature [29,77,86,93–96]. For example, Bao et al. [93] found that the degradation rate of BPA by nZVI supported on biochar was reduced (from 99.5% to 52.2%) when the initial pH of the solution was increased from 4 to 11, with a pH of 3 chosen as the optimal value. They also observed a similar performance for the BPA degradation in bare nZVI. Wei et al. [95] used *E. faecalis* in order to bio-recover Pd, which was then treated with Fe_3O_4 and nZVI to produce bio-Pd/Fe^0 attached to Fe_3O_4 nanoparticles for DCF degradation. According to their experiments conducted at a pH range of 3–9, they observed that acidic conditions favor DCF degradation. High degradation efficiencies of 94.69% and 99.65% in 20 min and 40 min, respectively, were obtained at pH 3, while they were very low at pH 7 and pH 9.

The pH adjustment to acidic values (3.5) enhanced the performance of the system, as evidenced by the higher ratio of mass of each compound removed per mass of R-nFe (Table 6). However, an increase in contact time from 2.2 to 4.4 min could not significantly enhance the removal ability and the process longevity of the system. As previously mentioned, acidic pH can trigger Fenton-like reactions, causing oxidation of the compounds. However, without the addition of an oxidative reagent the duration of this phenomenon is limited. For BPA, higher removal efficiencies were recorded on the first day of operation for both CT = 2.2 min (50%) and CT = 4.4 min (63%). On subsequent days, removal efficiencies decreased to 5% and 31% for CTs equal to 2.2 min and 4.4 min, respectively. For NSAIDs, the highest IBU and DCF removal efficiencies were obtained on the first day of operation. The IBU removal was 74% and 79% for CTs equal to 2.2 min and 4.4 min, respectively. The DCF removal was 81% and 86% for the two CT values investigated. Removal efficiencies followed the same trend for all the CECs studied and gradually decreased to values between 0% and 45% by the end of the experiments (Figure 4).

Table 6. The ratio of mass of pollutant removed per mass of the nanocomposite material (R-nFe) at the end of each experiment, with and without pH adjustment to 3.5 for the contact times of 2.2 min and 4.4 min (initial concentration of each pollutant, 5 μg/L).

Target Compound	Mass of Pollutant Removed per Mass of R-nFe (μg/g) at the End of Each Experiment (C_0 = 5 μg/L)			
	CT = 2.2 min, pH = 7	CT = 2.2 min, pH = 3.5	CT = 4.4 min, pH = 7	CT = 4.4 min, pH = 3.5
IBU	0.90	2.04	0.24	1.39
NPX	0.49	3.08	0.51	2.38
KFN	0.27	2.78	0.28	2.15
DCF	0.18	3.38	0.18	2.39
BPA	0.89	1.21	0.89	1.39

3.4. Oxidative Reagent Selection

Setting the inlet pH to acidic values (around 3.5) ameliorated the removal efficiency for most of the tested compounds, but for BPA and IBU it remained quite low. Within the context of this study, batch tests were carried out to evaluate the effect of H_2O_2 and PS sole addition on CECs removal, or combined with nZVI particles, as an activation agent.

The synergistic effect of R-nFe with the oxidative reagents appears to be a promising technology for the removal of CECs from water and wastewater. Many researchers

have investigated the synergy of nZVI with PS and H_2O_2 in batch tests performed either exclusively with each reagent [29,75,82,83,93,97,98] or with their combination [81,99]. Most publications reported that optimum results were obtained at an acidic pH of 3.

As shown in Figure 5, the control experiments showed that the two oxidative reagents alone could not effectively remove the target compounds, even at the highest concentration tested (3 mM) and the longest contact time (60 min). The effectiveness of the synergy between R-nFe material and oxidative reagent is quite high, especially for PS. The superiority of PS over H_2O_2 was recorded for DCF, BPA, and NPX. The removal efficiency of DCF and BPA was below 60% for R-nFe/H_2O_2 at all concentrations tested (1, 2, and 3 mM) for contact times of 30 and 60 min, respectively. On the other hand, even at the lowest dose of 1 mM, the addition of PS (R-nFe/PS system) achieved the removal of more than 80% of DCF at 30 min contact time and more than 70% of BPA after 60 min contact time. As can be seen in Figure 6, the removal of NPX by R-nFe/PS time was more than 80% after a 30 min contact time, while R-nFe/H_2O_2 contributed to the removal of almost 60–70% with no significant differences between the different doses tested. The simultaneous combination of H_2O_2 and PS with R-nFe showed a similar performance to the R-nFe/PS at 2 mM and achieved a high removal efficiency (more than 80%) for DCF, BPA, and NPX for both contact times tested (30 and 60 min). Furthermore, IBU and KFN recorded a moderate removal (about 50%) by R-nFe/PS at 1 mM for both of the tested contact times.

With the addition of H_2O_2, hydroxyl radicals (Equation (5)) could be formed by the divalent iron produced by nZVI oxidation (Equations (4), (6)–(8)) in a Fenton-like process, as described in previous section. Furthermore, in the presence of protons (H^+) and dissolved oxygen, H_2O_2 could also be generated as depicted in Equation (4).

The synergistic action of R-nFe with PS leads to the formation of sulfate radicals and possibly, to a lesser extent, hydroxyl radicals. Sulfate radicals can be formed directly (Equation (9)) or indirectly (Equations (10) and (11)) from nZVI if persulfate ions are present. Hydroxyl radicals can be formed by the reaction of sulfate radicals with hydroxyl groups (Equation (12)) or water (Equation (13)) [81] or by the direct reaction of nZVI with persulfate ions and water (Equation (14)) [29]. In addition, a heterogeneous Fenton reaction process is possible (Equations (4) and (5)). Both types of radicals ($SO_4^{\bullet-}$ and HO) are assumed to be present during the treatment process involving the addition of PS, with sulfate radicals predominating [29]. The degradation of pollutants by $SO_4^{\bullet-}$ is mainly by single-electron transfer, addition–elimination, and H-atom abstraction. The addition of HO to C=C leads to H-atom abstraction from C-H, N-H, or O-H [81]. The $SO_4^{\bullet-}$ radicals tend to react with the aromatic ring whereas HO reacts with both the aromatic ring and the aliphatic chain [100]. When combining H_2O_2 with PS, both radical species (HO and $SO_4^{\bullet-}$) are expected to play an important role.

$$Fe^0 + 2S_2O_8^{2-} \rightarrow Fe^{2+} + 2SO_4^{2-} + 2SO_4^{\bullet-} \quad (9)$$

$$Fe^0 + S_2O_8^{2-} \rightarrow Fe^{2+} + 2SO_4^{2-} \quad (10)$$

$$Fe^{2+} + S_2O_8^{2-} \rightarrow Fe^{3+} + SO_4^{2-} + SO_4^{\bullet-} \quad (11)$$

$$SO_4^{\bullet-} + OH^- \rightarrow HO + SO_4^{2-} \quad (12)$$

$$SO_4^{\bullet-} + H_2O \rightarrow SO_4^{2-} + HO + H^+ \quad (13)$$

$$Fe^0 + S_2O_8^{2-} + 2H_2O \rightarrow 2SO_4^{2-} + Fe^{2+} + 2HO + 2H^+ \quad (14)$$

Since PS addition seemed to be more efficient than H_2O_2 addition for the removal of most of the target compounds, it was decided to complement the nZVI system with the addition of a sodium persulfate solution.

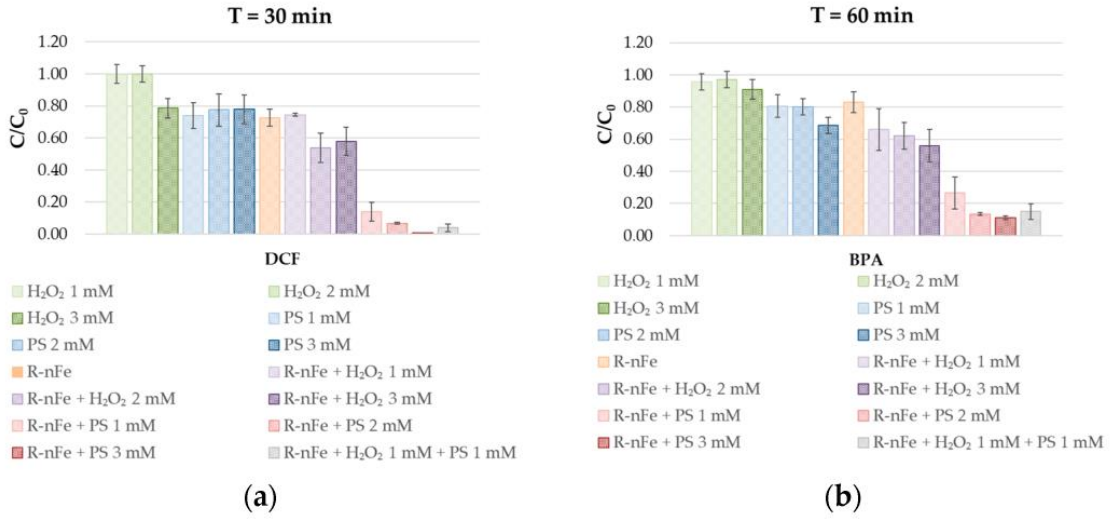

Figure 5. The removal efficiency of diclofenac at a contact time of 30 min (**a**) and bisphenol A at a contact time of 60 min (**b**) under different experimental conditions testing the effect of concentration of H_2O_2 and PS, their synergy with R-nFe, and a coupling of H_2O_2 with PS and R-nFe.

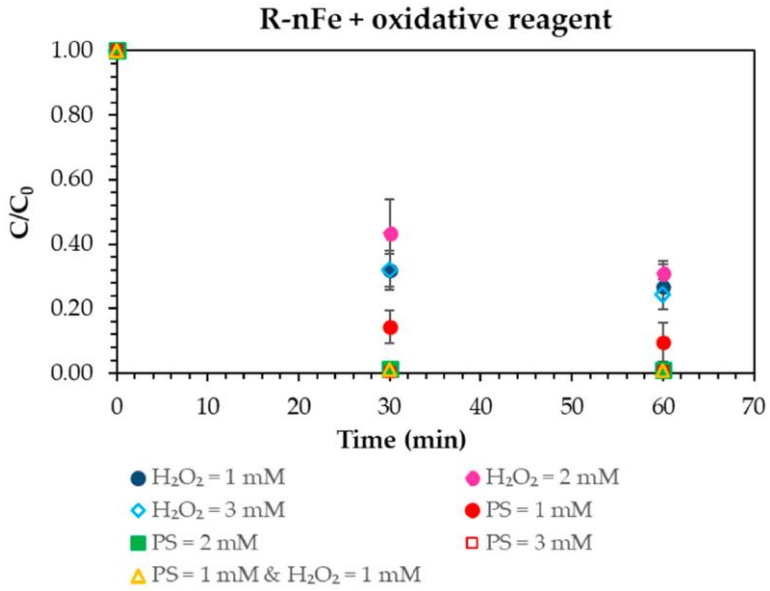

Figure 6. The synergistic effect of H_2O_2 and PS testing at three different concentrations (1, 2, and 3 mM) with R-nFe and their combination at a concentration of 1 mM each in the removal efficiency of naproxen.

3.5. Effect of PS Dose at Controlled pH

Taking into account the findings of the experiments presented in Sections 3.3 and 3.4, i.e., that the removal efficiency of the selected compounds is enhanced by acidic pH, while CT does not significantly affect removal and high removal rates could only be obtained by the synergistic effect of R-nFe with PS, it was decided to perform additional column experiments with a CT of 2.2 min, an acidic pH of 3.5, and PS addition. Two different PS concentrations (1 mM and 5 mM or 238 mg/L and 1191 mg/L) were investigated in the column set-up.

Figure 7 illustrates the effect of the PS concentration on the removal efficiency of DCF and BPA, while the graphs for the other compounds can be found in the Supplementary Materials (Figure S4). For IBU, the addition of 1 mM of PS resulted in steady, approximately 60% removal even after 250 h of operation. At the high PS dose (5 mM), the

removal efficiency remained around 80% throughout the experiment. In the case of NPX, BPA, and DCF, the system showed high removal efficiency, which was 80–90% throughout the experiment for both PS concentrations without significant differences, which can be attributed to the highly reactive SO_4^{-} free radicals. In contrast, KTP was not as readily degraded in wastewater, with average removal efficiencies of about 35% and 65% for PS 1 mM and PS 5 mM, respectively. With respect to the ratio of mass of the pollutant removed per mass of R-nFe, it is obvious that the addition of PS enhanced the performance of the system for all the studied substances, as illustrated in Table 7, indicating the importance of oxidation by radicals. For instance, the ratio for DCF compound removal increased to 6.70 μg DCF/g R-nFe with the addition of 1 mM PS, whereas the obtained removal without PS addition at the same contact time was equal to 0.18 and 3.38 μg DCF/g R-nFe at pH = 7 and 3.5, respectively. The improvement of CEC degradation achieved by coupling nZVI with PS has been studied in batch tests, as mentioned in Section 3.4, but this is the first time that the synergistic action of nZVI with PS is being evaluated in column tests for these recalcitrant organics. The results indicate that in the studied range of PS, the addition of a higher dose of PS (five times higher) did not significantly improve the removal efficiency or the longevity of the process for NPX, DCF, and BPA. As described in the previous section in detail, the main mechanisms involved in the removal of the target compounds are oxidation by sulfate radicals and possibly hydroxyl radicals, and adsorption on the surface of the (hydro)oxides of nZVI or in the resin pores.

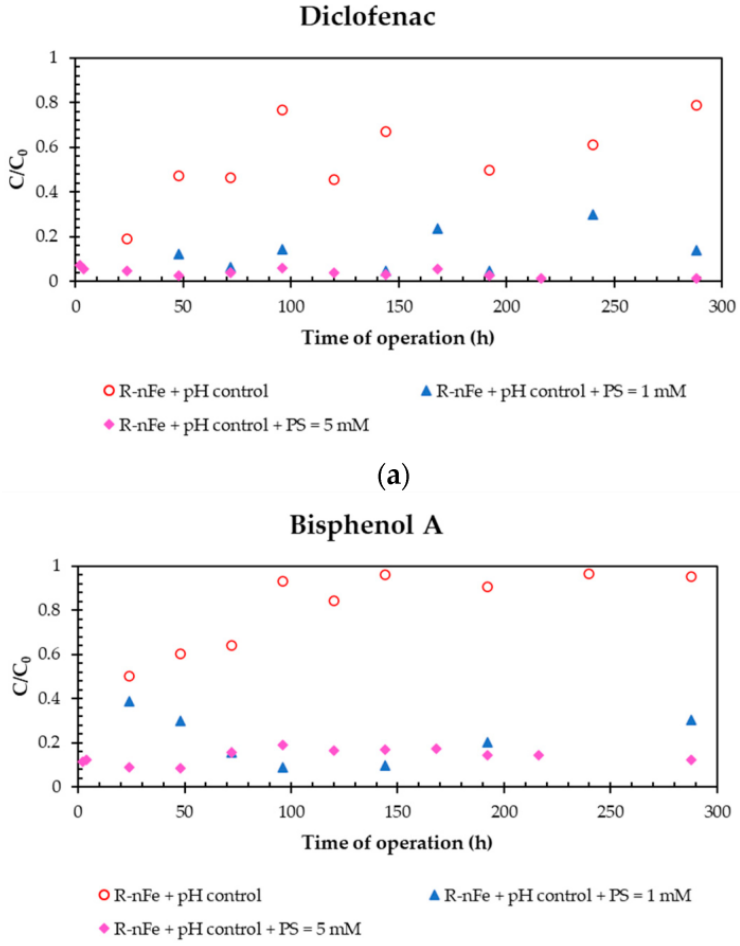

Figure 7. Effect of persulfate dose at controlled pH of the influent matrix to 3.5 on the removal efficiency of diclofenac (**a**) and bisphenol A (**b**) (Qwastewater = 26 L/d, Qpersulfate solution = 1.2 L/d, C_0 = 5 μg/L).

Table 7. The ratio of mass of pollutant removed per mass of the nanocomposite material (R-nFe) at the end of each experiment, testing two different sodium persulfate concentrations (initial concentration of each pollutant 5 μg/L, contact time 2.2 min, and pH adjustment to 3.5).

Target Compound	Mass of Pollutant Removed per Mass of R-nFe (μg/g) at the End of Each Experiment (C_0 = 5 μg/L, CT = 2.2 min)	
	PS = 1 mM	PS = 5 mM
IBU	3.87	6.74
NPX	7.14	7.32
KFN	2.72	5.02
DCF	6.70	7.56
BPA	6.01	6.70

4. Conclusions

The present work focused on proposing an integrated system for the removal of selected NSAIDs and an EDC in continuous flow column experiments. Based on the results, nZVI appears to be a promising technology for the removal of CECs from tertiary wastewater and could be used as a post-treatment method in WWTPs. This is the first time that nZVI has been studied and optimized for the removal of CECs in column tests assessing the longevity of the system's performance. It should be underlined that advanced treatment technologies are of increasing importance globally but also specifically in Europe, in view of the anticipated requirement for quaternary wastewater treatment in order to eliminate micro-pollutants that is included in the European Commission proposal (https://environment.ec.europa.eu/publications/proposal-revised-urban-wastewater-treatment-directive_en, accessed on 11 January 2023) for the revision of the Urban Wastewater Treatment Directive (UWWTD) 91/271/EEC.

According to the results, the optimum system's configuration consists of the nZVI column with pH adjustment of the influent at values around 3–3.5 and the addition of persulfate at a concentration of 1 mM. This configuration appeared to be very promising as it was able to achieve constantly high removals for almost all target compounds with values ranging between 70–99% for NPX, 70–95% for DCF, and 61–91% for BPA throughout the experiments, while IBU and KFN exhibited lower average removals of 58% and 35%, respectively. Future research should concentrate on the evaluation of the sustainability of the proposed system, mostly focusing on the regeneration of the resin. Furthermore, the pH control requirement of influent and effluent wastewater hinders the application and the cost efficiency of the process. Therefore, more studies are needed in order to evaluate the possibility of operating efficiently at higher pH values.

Supplementary Materials: The following supporting information can be downloaded at: https://www.mdpi.com/article/10.3390/w15030598/s1, Figure S1: Effect of initial concentration on the removal efficiency of Ibuprofen (a), Naproxen (b) and Ketoprofen (c) (Q = 26 L/d, CT = 8.8 min, no pH adjustment), Figure S2: Effect of contact time on the removal efficiency of Ibuprofen (a), Naproxen (b) and Ketoprofen (c) (Q = 26 L/d, C_0 = 5 μg/L, no pH adjustment), Figure S3: Effect of pH adjustment of the influent matrix to acidic values (approximately 3.5) and effect of contact time under acidic conditions on the removal efficiency of Ibuprofen (a), Naproxen (b) and Ketoprofen (c) (Q = 26 L/d, C_0 = 5 μg/L), Figure S4: Effect of persulfate dose at controlled pH of the influent matrix to 3.5 on the removal efficiency of Ibuprofen (a), Naproxen (b) and Ketoprofen (c) (Qwastewater = 26 L/d, Qpersulfate solution = 1.2 L/d, C_0 = 5 μg/L).

Author Contributions: Conceptualization, E.B. and C.N.; methodology, E.B., C.N. and D.M.; formal analysis, E.B. and M.K.; investigation, E.B. and I.P.; resources, C.N. and S.M.; data curation, E.B., A.G. and I.P.; writing—original draft preparation, E.B; writing—review and editing, C.N., D.M. and S.M.; visualization, E.K.; supervision, C.N.; project administration, C.N. and S.M.; funding acquisition, S.M. All authors have read and agreed to the published version of the manuscript.

Funding: This research was funded by the Partnership on Research and Innovation in the Mediterranean Area (PRIMA), within the project Safe and Sustainable Solutions for the Integrated Use of Non-Conventional Water Resources in the Mediterranean Agricultural Sector (FIT4REUSE), grant number [1823] [FIT4REUSE] [Call 2018 Section 1 Water]. The PRIMA Programme is supported under the Horizon 2020, the European Union's Framework Programme for Research and Innovation.

Data Availability Statement: This statement is excluded as no data are reported.

Acknowledgments: This study was carried out within the project "Safe and Sustainable Solutions for the Integrated Use of Non-Conventional Water Resources in the Mediterranean Agricultural Sector (FIT4REUSE)" which has received funding from the Partnership on Research and Innovation in the Mediterranean Area (PRIMA) under grant agreement No. 1823. PRIMA is supported by the European Union's Horizon 2020 research and innovation program.

Conflicts of Interest: The authors declare no conflict of interest.

References

1. Geissen, V.; Mol, H.; Klumpp, E.; Umlauf, G.; Nadal, M.; van der Ploeg, M.; van de Zee, S.E.A.T.M.; Ritsema, C.J. Emerging Pollutants in the Environment: A Challenge for Water Resource Management. *Int. Soil Water Conserv. Res.* **2015**, *3*, 57–65. [CrossRef]
2. Abdulrazaq, Y.; Abdulsalam, A.; Larayetan Rotimi, A.; Aliyu Abdulbasit, A.; Clifford, O.; Abdulazeez Abdulsalam, O.; Nayo Racheal, O.; Akor Joy, A.; Omale Victor, F.; Mbese Johannes, Z.; et al. Classification, Potential Routes and Risk of Emerging Pollutants/Contaminant. In *Emerging Contaminants*; Nuro, A., Ed.; IntechOpen: London, UK, 2021; ISBN 978-1-83962-418-6.
3. Arman, N.Z.; Salmiati, S.; Aris, A.; Salim, M.R.; Nazifa, T.H.; Muhamad, M.S.; Marpongahtun, M. A Review on Emerging Pollutants in the Water Environment: Existences, Health Effects and Treatment Processes. *Water* **2021**, *13*, 3258. [CrossRef]
4. Sivaranjanee, R.; Kumar, P.S. A Review on Remedial Measures for Effective Separation of Emerging Contaminants from Wastewater. *Environ. Technol. Innov.* **2021**, *23*, 101741. [CrossRef]
5. López-Pacheco, I.Y.; Silva-Núñez, A.; Salinas-Salazar, C.; Arévalo-Gallegos, A.; Lizarazo-Holguin, L.A.; Barceló, D.; Iqbal, H.M.N.; Parra-Saldívar, R. Anthropogenic Contaminants of High Concern: Existence in Water Resources and Their Adverse Effects. *Sci. Total Environ.* **2019**, *690*, 1068–1088. [CrossRef] [PubMed]
6. la Farré, M.; Pérez, S.; Kantiani, L.; Barceló, D. Fate and Toxicity of Emerging Pollutants, Their Metabolites and Transformation Products in the Aquatic Environment. *TrAC Trends Anal. Chem.* **2008**, *27*, 991–1007. [CrossRef]
7. Caliman, F.A.; Gavrilescu, M. Pharmaceuticals, Personal Care Products and Endocrine Disrupting Agents in the Environment—A Review. *Clean Soil Air Water* **2009**, *37*, 277–303. [CrossRef]
8. Świacka, K.; Michnowska, A.; Maculewicz, J.; Caban, M.; Smolarz, K. Toxic Effects of NSAIDs in Non-Target Species: A Review from the Perspective of the Aquatic Environment. *Environ. Pollut.* **2021**, *273*, 115891. [CrossRef]
9. Gao, X.; Kang, S.; Xiong, R.; Chen, M. Environment-Friendly Removal Methods for Endocrine Disrupting Chemicals. *Sustainability* **2020**, *12*, 7615. [CrossRef]
10. Gross-Sorokin, M.Y.; Roast, S.D.; Brighty, G.C. Assessment of Feminization of Male Fish in English Rivers by the Environment Agency of England and Wales. *Environ. Health Perspect.* **2006**, *114*, 147–151. [CrossRef]
11. Hayes, T.B.; Anderson, L.L.; Beasley, V.R.; de Solla, S.R.; Iguchi, T.; Ingraham, H.; Kestemont, P.; Kniewald, J.; Kniewald, Z.; Langlois, V.S.; et al. Demasculinization and Feminization of Male Gonads by Atrazine: Consistent Effects across Vertebrate Classes. *J. Steroid Biochem. Mol. Biol.* **2011**, *127*, 64–73. [CrossRef]
12. Zha, J.; Sun, L.; Spear, P.A.; Wang, Z. Comparison of Ethinylestradiol and Nonylphenol Effects on Reproduction of Chinese Rare Minnows (Gobiocypris Rarus). *Ecotoxicol. Environ. Saf.* **2008**, *71*, 390–399. [CrossRef]
13. Ji, H.; Song, N.; Ren, J.; Li, W.; Xu, B.; Li, H.; Shen, G. Metabonomics Reveals Bisphenol A Affects Fatty Acid and Glucose Metabolism through Activation of LXR in the Liver of Male Mice. *Sci. Total Environ.* **2020**, *703*, 134681. [CrossRef] [PubMed]
14. Huang, Q.; Chen, Y.; Lin, L.; Liu, Y.; Chi, Y.; Lin, Y.; Ye, G.; Zhu, H.; Dong, S. Different Effects of Bisphenol a and Its Halogenated Derivatives on the Reproduction and Development of Oryzias Melastigma under Environmentally Relevant Doses. *Sci. Total Environ.* **2017**, *595*, 752–758. [CrossRef] [PubMed]
15. Marcial, H.S.; Hagiwara, A.; Snell, T.W. Estrogenic Compounds Affect Development of Harpacticoid Copepod Tigriopus Japonicus. *Environ. Toxicol Chem* **2003**, *22*, 3025. [CrossRef]
16. O'Connor, J.C.; Chapin, R.E. Critical Evaluation of Observed Adverse Effects of Endocrine Active Substances on Reproduction and Development, the Immune System, and the Nervous System. *Pure Appl. Chem.* **2003**, *75*, 2099–2123. [CrossRef]
17. Priyanka; Trivedi, A.; Maske, P.; Mote, C.; Dighe, V. Gestational and Lactational Exposure to Triclosan Causes Impaired Fertility of F1 Male Offspring and Developmental Defects in F2 Generation. *Environ. Pollut.* **2020**, *257*, 113617. [CrossRef] [PubMed]
18. Tabari, S.A.; Esfahani, M.L.; Hosseini, S.M.; Rahimi, A. Neurobehavioral Toxicity of Triclosan in Mice. *Food Chem. Toxicol.* **2019**, *130*, 154–160. [CrossRef]
19. da Silva, T.L.; Costa, C.S.D.; da Silva, M.G.C.; Vieira, M.G.A. Overview of Non-Steroidal Anti-Inflammatory Drugs Degradation by Advanced Oxidation Processes. *J. Clean. Prod.* **2022**, *346*, 131226. [CrossRef]

20. Azizi, D.; Arif, A.; Blair, D.; Dionne, J.; Filion, Y.; Ouarda, Y.; Pazmino, A.G.; Pulicharla, R.; Rilstone, V.; Tiwari, B.; et al. A Comprehensive Review on Current Technologies for Removal of Endocrine Disrupting Chemicals from Wastewaters. *Environ. Res.* **2022**, *207*, 112196. [CrossRef] [PubMed]
21. Rastogi, A.; Tiwari, M.K.; Ghangrekar, M.M. A Review on Environmental Occurrence, Toxicity and Microbial Degradation of Non-Steroidal Anti-Inflammatory Drugs (NSAIDs). *J. Environ. Manag.* **2021**, *300*, 113694. [CrossRef]
22. de Andrade, J.R.; Oliveira, M.F.; Canevesi, R.L.S.; Landers, R.; da Silva, M.G.C.; Vieira, M.G.A. Comparative Adsorption of Diclofenac Sodium and Losartan Potassium in Organophilic Clay-Packed Fixed-Bed: X-Ray Photoelectron Spectroscopy Characterization, Experimental Tests and Theoretical Study on DFT-Based Chemical Descriptors. *J. Mol. Liq.* **2020**, *312*, 113427. [CrossRef]
23. Park, Y.; Ayoko, G.A.; Frost, R.L. Application of Organoclays for the Adsorption of Recalcitrant Organic Molecules from Aqueous Media. *J. Colloid Interface Sci.* **2011**, *354*, 292–305. [CrossRef] [PubMed]
24. Jedynak, K.; Szczepanik, B.; Rędzia, N.; Słomkiewicz, P.; Kolbus, A.; Rogala, P. Ordered Mesoporous Carbons for Adsorption of Paracetamol and Non-Steroidal Anti-Inflammatory Drugs: Ibuprofen and Naproxen from Aqueous Solutions. *Water* **2019**, *11*, 1099. [CrossRef]
25. Streit, A.F.M.; Collazzo, G.C.; Druzian, S.P.; Verdi, R.S.; Foletto, E.L.; Oliveira, L.F.S.; Dotto, G.L. Adsorption of Ibuprofen, Ketoprofen, and Paracetamol onto Activated Carbon Prepared from Effluent Treatment Plant Sludge of the Beverage Industry. *Chemosphere* **2021**, *262*, 128322. [CrossRef]
26. Sui, Q.; Huang, J.; Liu, Y.; Chang, X.; Ji, G.; Deng, S.; Xie, T.; Yu, G. Rapid Removal of Bisphenol A on Highly Ordered Mesoporous Carbon. *J. Environ. Sci.* **2011**, *23*, 177–182. [CrossRef] [PubMed]
27. Ma, D.; Yi, H.; Lai, C.; Liu, X.; Huo, X.; An, Z.; Li, L.; Fu, Y.; Li, B.; Zhang, M.; et al. Critical Review of Advanced Oxidation Processes in Organic Wastewater Treatment. *Chemosphere* **2021**, *275*, 130104. [CrossRef]
28. Wang, J.; Wang, S. Activation of Persulfate (PS) and Peroxymonosulfate (PMS) and Application for the Degradation of Emerging Contaminants. *Chem. Eng. J.* **2018**, *334*, 1502–1517. [CrossRef]
29. Hussain, I.; Li, M.; Zhang, Y.; Li, Y.; Huang, S.; Du, X.; Liu, G.; Hayat, W.; Anwar, N. Insights into the Mechanism of Persulfate Activation with NZVI/BC Nanocomposite for the Degradation of Nonylphenol. *Chem. Eng. J.* **2017**, *311*, 163–172. [CrossRef]
30. Gomes, J.; Costa, R.; Quinta-Ferreira, R.M.; Martins, R.C. Application of Ozonation for Pharmaceuticals and Personal Care Products Removal from Water. *Sci. Total Environ.* **2017**, *586*, 265–283. [CrossRef]
31. Ning, B.; Graham, N.; Zhang, Y.; Nakonechny, M.; Gamal El-Din, M. Degradation of Endocrine Disrupting Chemicals by Ozone/AOPs. *Ozone Sci. Eng.* **2007**, *29*, 153–176. [CrossRef]
32. Wang, J.; Chen, H. Catalytic Ozonation for Water and Wastewater Treatment: Recent Advances and Perspective. *Sci. Total Environ.* **2020**, *704*, 135249. [CrossRef] [PubMed]
33. He, Y.; Sutton, N.B.; Rijnaarts, H.H.H.; Langenhoff, A.A.M. Degradation of Pharmaceuticals in Wastewater Using Immobilized TiO_2 Photocatalysis under Simulated Solar Irradiation. *Appl. Catal. B Environ.* **2016**, *182*, 132–141. [CrossRef]
34. Kaur, A.; Umar, A.; Kansal, S.K. Sunlight-Driven Photocatalytic Degradation of Non-Steroidal Anti-Inflammatory Drug Based on TiO_2 Quantum Dots. *J. Colloid Interface Sci.* **2015**, *459*, 257–263. [CrossRef] [PubMed]
35. Vela, N.; Calín, M.; Yáñez-Gascón, M.J.; Garrido, I.; Pérez-Lucas, G.; Fenoll, J.; Navarro, S. Photocatalytic Oxidation of Six Pesticides Listed as Endocrine Disruptor Chemicals from Wastewater Using Two Different TiO2 Samples at Pilot Plant Scale under Sunlight Irradiation. *J. Photochem. Photobiol. A Chem.* **2018**, *353*, 271–278. [CrossRef]
36. Villanueva-Rodríguez, M.; Bello-Mendoza, R.; Hernández-Ramírez, A.; Ruiz-Ruiz, E.J. Degradation of Anti-Inflammatory Drugs in Municipal Wastewater by Heterogeneous Photocatalysis and Electro-Fenton Process. *Environ. Technol.* **2019**, *40*, 2436–2445. [CrossRef]
37. Zatloukalová, K.; Obalová, L.; Koči, K.; Čapek, L.; Matěj, Z.; Šnajdhaufová, H.; Ryczkowski, J.; Słowik, G. Photocatalytic Degradation of Endocrine Disruptor Compounds in Water over Immobilized TiO2 Photocatalysts. *Iran. J. Chem. Chem. Eng.* **2017**, *36*, 29–38. [CrossRef]
38. Augsburger, N.; Zaouri, N.; Cheng, H.; Hong, P.-Y. The Use of UV/H2O2 to Facilitate Removal of Emerging Contaminants in Anaerobic Membrane Bioreactor Effluents. *Environ. Res.* **2021**, *198*, 110479. [CrossRef]
39. Wang, P.; Bu, L.; Wu, Y.; Ma, W.; Zhu, S.; Zhou, S. Mechanistic Insight into the Degradation of Ibuprofen in UV/H2O2 Process via a Combined Experimental and DFT Study. *Chemosphere* **2021**, *267*, 128883. [CrossRef]
40. Jain, B.; Singh, A.K.; Kim, H.; Lichtfouse, E.; Sharma, V.K. Treatment of Organic Pollutants by Homogeneous and Heterogeneous Fenton Reaction Processes. *Environ. Chem. Lett.* **2018**, *16*, 947–967. [CrossRef]
41. Adityosulindro, S.; Barthe, L.; González-Labrada, K.; Jáuregui Haza, U.J.; Delmas, H.; Julcour, C. Sonolysis and Sono-Fenton Oxidation for Removal of Ibuprofen in (Waste)Water. *Ultrason. Sonochem.* **2017**, *39*, 889–896. [CrossRef]
42. Camargo-Perea, A.L.; Rubio-Clemente, A.; Peñuela, G.A. Use of Ultrasound as an Advanced Oxidation Process for the Degradation of Emerging Pollutants in Water. *Water* **2020**, *12*, 1068. [CrossRef]
43. Peng, J.; Wang, Z.; Wang, S.; Liu, J.; Zhang, Y.; Wang, B.; Gong, Z.; Wang, M.; Dong, H.; Shi, J.; et al. Enhanced Removal of Methylparaben Mediated by Cobalt/Carbon Nanotubes (Co/CNTs) Activated Peroxymonosulfate in Chloride-Containing Water: Reaction Kinetics, Mechanisms and Pathways. *Chem. Eng. J.* **2021**, *409*, 128176. [CrossRef]

44. Dai, Y.; Cao, H.; Qi, C.; Zhao, Y.; Wen, Y.; Xu, C.; Zhong, Q.; Sun, D.; Zhou, S.; Yang, B.; et al. L-Cysteine Boosted Fe(III)-Activated Peracetic Acid System for Sulfamethoxazole Degradation: Role of L-Cysteine and Mechanism. *Chem. Eng. J.* **2023**, *451*, 138588. [CrossRef]
45. Dai, Y.; Qi, C.; Cao, H.; Wen, Y.; Zhao, Y.; Xu, C.; Yang, S.; He, H. Enhanced Degradation of Sulfamethoxazole by Microwave-Activated Peracetic Acid under Alkaline Condition: Influencing Factors and Mechanism. *Sep. Purif. Technol.* **2022**, *288*, 120716. [CrossRef]
46. Baldermann, A.; Kaufhold, S.; Dohrmann, R.; Baldermann, C.; Letofsky-Papst, I.; Dietzel, M. A Novel NZVI–Bentonite Nanocomposite to Remove Trichloroethene (TCE) from Solution. *Chemosphere* **2021**, *282*, 131018. [CrossRef]
47. Gu, M.; Farooq, U.; Lu, S.; Zhang, X.; Qiu, Z.; Sui, Q. Degradation of Trichloroethylene in Aqueous Solution by RGO Supported NZVI Catalyst under Several Oxic Environments. *J. Hazard. Mater.* **2018**, *349*, 35–44. [CrossRef]
48. Huang, L.; Weng, X.; Chen, Z.; Megharaj, M.; Naidu, R. Green Synthesis of Iron Nanoparticles by Various Tea Extracts: Comparative Study of the Reactivity. *Spectrochim. Acta Part A Mol. Biomol. Spectrosc.* **2014**, *130*, 295–301. [CrossRef] [PubMed]
49. Raman, C.D.; Kanmani, S. Textile Dye Degradation Using Nano Zero Valent Iron: A Review. *J. Environ. Manag.* **2016**, *177*, 341–355. [CrossRef]
50. Fazlzadeh, M.; Rahmani, K.; Zarei, A.; Abdoallahzadeh, H.; Nasiri, F.; Khosravi, R. A Novel Green Synthesis of Zero Valent Iron Nanoparticles (NZVI) Using Three Plant Extracts and Their Efficient Application for Removal of Cr(VI) from Aqueous Solutions. *Adv. Powder Technol.* **2017**, *28*, 122–130. [CrossRef]
51. Selvan, B.K.; Thiyagarajan, K.; Das, S.; Jaya, N.; Jabasingh, S.A.; Saravanan, P.; Rajasimman, M.; Vasseghian, Y. Synthesis and Characterization of Nano Zerovalent Iron-Kaolin Clay (NZVI-Kaol) Composite Polyethersulfone (PES) Membrane for the Efficacious As2O3 Removal from Potable Water Samples. *Chemosphere* **2022**, *288*, 132405. [CrossRef]
52. Toli, A.; Varouxaki, A.; Mystrioti, C.; Xenidis, A.; Papassiopi, N. Green Synthesis of Resin Supported Nanoiron and Evaluation of Efficiency for the Remediation of Cr(VI) Contaminated Groundwater by Batch Tests. *Bull. Environ. Contam. Toxicol.* **2018**, *101*, 711–717. [CrossRef] [PubMed]
53. Singh, S.P.; Bose, P. Degradation Kinetics of Endosulfan Isomers by Micron- and Nano-Sized Zero Valent Iron Particles (MZVI and NZVI): Degradation Kinetics of Endosulfan Isomers. *J. Chem. Technol. Biotechnol.* **2016**, *91*, 2313–2321. [CrossRef]
54. Thompson, J.M.; Chisholm, B.J.; Bezbaruah, A.N. Reductive Dechlorination of Chloroacetanilide Herbicide (Alachlor) Using Zero-Valent Iron Nanoparticles. *Environ. Eng. Sci.* **2010**, *27*, 227–232. [CrossRef]
55. Wang, X.; Deng, R.; Shen, W.; Huang, J.; Li, Q.; Zhao, Y.; Wan, J.; Zhou, Y.; Long, T.; Zhang, S. Rapid Degradation of Nitrochlorobenzene by Activated Persulfate Oxidation With Biochar Supported Nanoscaled Zero Valent Iron. *Front. Chem.* **2021**, *9*, 615694. [CrossRef] [PubMed]
56. Haneef, T.; Ul Mustafa, M.R.; Rasool, K.; Ho, Y.C.; Mohamed Kutty, S.R. Removal of Polycyclic Aromatic Hydrocarbons in a Heterogeneous Fenton Like Oxidation System Using Nanoscale Zero-Valent Iron as a Catalyst. *Water* **2020**, *12*, 2430. [CrossRef]
57. Baig, N.; Kammakakam, I.; Falath, W. Nanomaterials: A Review of Synthesis Methods, Properties, Recent Progress, and Challenges. *Mater. Adv.* **2021**, *2*, 1821–1871. [CrossRef]
58. Khatir, N.M.; Sabbagh, F. Green Facile Synthesis of Silver-Doped Zinc Oxide Nanoparticles and Evaluation of Their Effect on Drug Release. *Materials* **2022**, *15*, 5536. [CrossRef] [PubMed]
59. Mahmoudi Khatir, N.; Abdul-Malek, Z.; Zak, A.K.; Akbari, A.; Sabbagh, F. Sol–Gel Grown Fe-Doped ZnO Nanoparticles: Antibacterial and Structural Behaviors. *J. Sol-Gel Sci. Technol.* **2016**, *78*, 91–98. [CrossRef]
60. Bruns, J.; Gheorghiu, F.; Borda, M.; Bosch, J. Experiences from Pilot- and Large-Scale Demonstration Sites from Across the Globe Including Combined Remedies with NZVI. In *Nanoscale Zerovalent Iron Particles for Environmental Restoration*; Phenrat, T., Lowry, G.V., Eds.; Springer International Publishing: Cham, Switzerland, 2019; pp. 335–357. ISBN 978-3-319-95338-0.
61. Chanthapon, N.; Sarkar, S.; Kidkhunthod, P.; Padungthon, S. Lead Removal by a Reusable Gel Cation Exchange Resin Containing Nano-Scale Zero Valent Iron. *Chem. Eng. J.* **2018**, *331*, 545–555. [CrossRef]
62. Li, S.; Wang, W.; Liu, Y.; Zhang, W. Zero-Valent Iron Nanoparticles (NZVI) for the Treatment of Smelting Wastewater: A Pilot-Scale Demonstration. *Chem. Eng. J.* **2014**, *254*, 115–123. [CrossRef]
63. Němeček, J.; Lhotský, O.; Cajthaml, T. Nanoscale Zero-Valent Iron Application for in Situ Reduction of Hexavalent Chromium and Its Effects on Indigenous Microorganism Populations. *Sci. Total Environ.* **2014**, *485–486*, 739–747. [CrossRef] [PubMed]
64. Ponder, S.M.; Darab, J.G.; Mallouk, T.E. Remediation of Cr(VI) and Pb(II) Aqueous Solutions Using Supported, Nanoscale Zero-Valent Iron. *Environ. Sci. Technol.* **2000**, *34*, 2564–2569. [CrossRef]
65. Tarekegn, M.M.; Hiruy, A.M.; Dekebo, A.H. Nano Zero Valent Iron (NZVI) Particles for the Removal of Heavy Metals (Cd^{2+}, Cu^{2+} and Pb^{2+}) from Aqueous Solutions. *RSC Adv.* **2021**, *11*, 18539–18551. [CrossRef]
66. Toli, A.; Mystrioti, C.; Avgoustidis, I.; Papassiopi, N. Fixed-Bed Flow Experiments with Supported Green NZVI for the Remediation of Contaminated Waters: Effect of PH and Background Solution Composition. *Chemosphere* **2021**, *279*, 130472. [CrossRef]
67. Sheu, Y.T.; Lien, P.J.; Chen, K.F.; Ou, J.H.; Kao, C.M. Application of NZVI-Contained Emulsified Substrate to Bioremediate PCE-Contaminated Groundwater—A Pilot-Scale Study. *Chem. Eng. J.* **2016**, *304*, 714–727. [CrossRef]
68. Song, Y.; Fang, G.; Zhu, C.; Zhu, F.; Wu, S.; Chen, N.; Wu, T.; Wang, Y.; Gao, J.; Zhou, D. Zero-Valent Iron Activated Persulfate Remediation of Polycyclic Aromatic Hydrocarbon-Contaminated Soils: An in Situ Pilot-Scale Study. *Chem. Eng. J.* **2019**, *355*, 65–75. [CrossRef]

69. Mdlovu, N.V.; Lin, K.-S.; Hsien, M.-J.; Chang, C.-J.; Kunene, S.C. Synthesis, Characterization, and Application of Zero-Valent Iron Nanoparticles for TNT, RDX, and HMX Explosives Decontamination in Wastewater. *J. Taiwan Inst. Chem. Eng.* **2020**, *114*, 186–198. [CrossRef]
70. Jerold, M.; Joseph, D.; Patra, N.; Sivasubramanian, V. Fixed-Bed Column Studies for the Removal of Hazardous Malachite Green Dye from Aqueous Solution Using Novel Nano Zerovalent Iron Algal Biocomposite. *Nanotechnol. Environ. Eng.* **2016**, *1*, 8. [CrossRef]
71. Zhao, Z.; Liu, J.; Tai, C.; Zhou, Q.; Hu, J.; Jiang, G. Rapid Decolorization of Water Soluble Azo-Dyes by Nanosized Zero-Valent Iron Immobilized on the Exchange Resin. *Sci. China Ser. B-Chem.* **2008**, *51*, 186–192. [CrossRef]
72. Makhathini, T.P.; Mulopo, J.; Bakare, B.F. Enriched Co-Treatment of Pharmaceutical and Acidic Metal-Containing Wastewater with Nano Zero-Valent Iron. *Minerals* **2021**, *11*, 220. [CrossRef]
73. Sulaiman, S.M.; Al-Jabari, M.H. Enhanced Adsorptive Removal of Diclofenac Sodium from Aqueous Solution by Bentonite-Supported Nanoscale Zero-Valent Iron. *Arab J. Basic Appl. Sci.* **2021**, *28*, 51–63. [CrossRef]
74. Esmaeili Bidhendi, M.; Parandi, E.; Mahmoudi Meymand, M.; Sereshti, H.; Rashidi Nodeh, H.; Joo, S.-W.; Vasseghian, Y.; Mahmoudi Khatir, N.; Rezania, S. Removal of Lead Ions from Wastewater Using Magnesium Sulfide Nanoparticles Caged Alginate Microbeads. *Environ. Res.* **2023**, *216*, 114416. [CrossRef]
75. Girit, B.; Dursun, D.; Olmez-Hanci, T.; Arslan-Alaton, I. Treatment of Aqueous Bisphenol A Using Nano-Sized Zero-Valent Iron in the Presence of Hydrogen Peroxide and Persulfate Oxidants. *Water Sci. Technol.* **2015**, *71*, 1859–1868. [CrossRef] [PubMed]
76. Tyumina, E.A.; Bazhutin, G.A.; Cartagena Gómez, A.d.P.; Ivshina, I.B. Nonsteroidal Anti-Inflammatory Drugs as Emerging Contaminants. *Microbiology* **2020**, *89*, 148–163. [CrossRef]
77. Panagou, I.; Noutsopoulos, C.; Mystrioti, C.; Barka, E.; Koumaki, E.; Kalli, M.; Malamis, S.; Papassiopi, N.; Mamais, D. Assessing the Performance of Environmentally Friendly-Produced Zerovalent Iron Nanoparticles to Remove Pharmaceuticals from Water. *Sustainability* **2021**, *13*, 12708. [CrossRef]
78. Tran, N.H.; Reinhard, M.; Gin, K.Y.-H. Occurrence and Fate of Emerging Contaminants in Municipal Wastewater Treatment Plants from Different Geographical Regions-a Review. *Water Res.* **2018**, *133*, 182–207. [CrossRef] [PubMed]
79. Flint, S.; Markle, T.; Thompson, S.; Wallace, E. Bisphenol A Exposure, Effects, and Policy: A Wildlife Perspective. *J. Environ. Manag.* **2012**, *104*, 19–34. [CrossRef]
80. Gao, F.; Li, Y.; Xiang, B. Degradation of Bisphenol A through Transition Metals Activating Persulfate Process. *Ecotoxicol. Environ. Saf.* **2018**, *158*, 239–247. [CrossRef]
81. Wu, J.; Wang, B.; Cagnetta, G.; Huang, J.; Wang, Y.; Deng, S.; Yu, G. Nanoscale Zero Valent Iron-Activated Persulfate Coupled with Fenton Oxidation Process for Typical Pharmaceuticals and Personal Care Products Degradation. *Sep. Purif. Technol.* **2020**, *239*, 116534. [CrossRef]
82. Gao, Y.; Gao, N.; Wang, W.; Kang, S.; Xu, J.; Xiang, H.; Yin, D. Ultrasound-Assisted Heterogeneous Activation of Persulfate by Nano Zero-Valent Iron (NZVI) for the Propranolol Degradation in Water. *Ultrason. Sonochem.* **2018**, *49*, 33–40. [CrossRef]
83. Gao, J.; Han, D.; Xu, Y.; Liu, Y.; Shang, J. Persulfate Activation by Sulfide-Modified Nanoscale Iron Supported by Biochar (S-NZVI/BC) for Degradation of Ciprofloxacin. *Sep. Purif. Technol.* **2020**, *235*, 116202. [CrossRef]
84. Samaras, V.G.; Thomaidis, N.S.; Stasinakis, A.S.; Lekkas, T.D. An Analytical Method for the Simultaneous Trace Determination of Acidic Pharmaceuticals and Phenolic Endocrine Disrupting Chemicals in Wastewater and Sewage Sludge by Gas Chromatography-Mass Spectrometry. *Anal. Bioanal. Chem.* **2011**, *399*, 2549–2561. [CrossRef] [PubMed]
85. Ali, I.; Afshinb, S.; Poureshgh, Y.; Azari, A.; Rashtbari, Y.; Feizizadeh, A.; Hamzezadeh, A.; Fazlzadeh, M. Green Preparation of Activated Carbon from Pomegranate Peel Coated with Zero-Valent Iron Nanoparticles (NZVI) and Isotherm and Kinetic Studies of Amoxicillin Removal in Water. *Environ. Sci. Pollut. Res.* **2020**, *27*, 36732–36743. [CrossRef] [PubMed]
86. Dehghani, M.H.; Karri, R.R.; Alimohammadi, M.; Nazmara, S.; Zarei, A.; Saeedi, Z. Insights into Endocrine-Disrupting Bisphenol-A Adsorption from Pharmaceutical Effluent by Chitosan Immobilized Nanoscale Zero-Valent Iron Nanoparticles. *J. Mol. Liq.* **2020**, *311*, 113317. [CrossRef]
87. Soares, S.F.; Trindade, T.; Daniel-da-Silva, A.L. Enhanced Removal of Non-Steroidal Inflammatory Drugs from Water by Quaternary Chitosan-Based Magnetic Nanosorbents. *Coatings* **2021**, *11*, 964. [CrossRef]
88. Senin, R.; Ion, I.; Ion, A. A Sorption Study of Bisphenol A in AqueousSolutions on Pristine and Oxidized Multi-WalledCarbon Nanotubes. *Pol. J. Environ. Stud.* **2018**, *27*, 2245–2257. [CrossRef] [PubMed]
89. Wang, S.; Gao, B.; Li, Y.; Creamer, A.E.; He, F. Adsorptive Removal of Arsenate from Aqueous Solutions by Biochar Supported Zero-Valent Iron Nanocomposite: Batch and Continuous Flow Tests. *J. Hazard. Mater.* **2017**, *322*, 172–181. [CrossRef]
90. Eljamal, O. Continuous-Flow of Nanoscale Zero Valent Iron Based System for Phosphorus Removal. 2021.
91. Rezaei, F.; Vione, D. Effect of PH on Zero Valent Iron Performance in Heterogeneous Fenton and Fenton-Like Processes: A Review. *Molecules* **2018**, *23*, 3127. [CrossRef]
92. Liu, X.; Cao, Z.; Yuan, Z.; Zhang, J.; Guo, X.; Yang, Y.; He, F.; Zhao, Y.; Xu, J. Insight into the Kinetics and Mechanism of Removal of Aqueous Chlorinated Nitroaromatic Antibiotic Chloramphenicol by Nanoscale Zero-Valent Iron. *Chem. Eng. J.* **2018**, *334*, 508–518. [CrossRef]
93. Bao, T.; Damtie, M.M.; Hosseinzadeh, A.; Wei, W.; Jin, J.; Phong Vo, H.N.; Ye, J.S.; Liu, Y.; Wang, X.F.; Yu, Z.M.; et al. Bentonite-Supported Nano Zero-Valent Iron Composite as a Green Catalyst for Bisphenol A Degradation: Preparation, Performance, and Mechanism of Action. *J. Environ. Manag.* **2020**, *260*, 110105. [CrossRef]

94. Gao, J.-F.; Wu, Z.-L.; Duan, W.-J.; Zhang, W.-Z. Simultaneous Adsorption and Degradation of Triclosan by Ginkgo Biloba L. Stabilized Fe/Co Bimetallic Nanoparticles. *Sci. Total Environ.* **2019**, *662*, 978–989. [CrossRef] [PubMed]
95. Wei, X.; Zhu, N.; Huang, X.; Kang, N.; Wu, P.; Dang, Z. Efficient Degradation of Sodium Diclofenac via Heterogeneous Fenton Reaction Boosted by Pd/Fe@Fe_3O_4 Nanoparticles Derived from Bio-Recovered Palladium. *J. Environ. Manag.* **2020**, *260*, 110072. [CrossRef] [PubMed]
96. Ziylan, A.; Koltypin, Y.; Gedanken, A.; Ince, N.H. More on Sonolytic and Sonocatalytic Decomposition of Diclofenac Using Zero-Valent Iron. *Ultrason. Sonochem.* **2013**, *20*, 580–586. [CrossRef]
97. Daneshkhah, M.; Hossaini, H.; Malakootian, M. Removal of Metoprolol from Water by Sepiolite-Supported Nanoscale Zero-Valent Iron. *J. Environ. Chem. Eng.* **2017**, *5*, 3490–3499. [CrossRef]
98. Mondal, S.K.; Saha, A.K.; Sinha, A. Removal of Ciprofloxacin Using Modified Advanced Oxidation Processes: Kinetics, Pathways and Process Optimization. *J. Clean. Prod.* **2018**, *171*, 1203–1214. [CrossRef]
99. Dogan, M.; Ozturk, T.; Olmez-Hanci, T.; Arslan-Alaton, I. Persulfate and Hydrogen Peroxide-Activated Degradation of Bisphenol A with Nano-Scale Zero-Valent Iron and Aluminum. *J. Adv. Oxid. Technol.* **2016**, *19*, 266–275. [CrossRef]
100. Choi, J.; Cui, M.; Lee, Y.; Kim, J.; Son, Y.; Khim, J. Hydrodynamic Cavitation and Activated Persulfate Oxidation for Degradation of Bisphenol A: Kinetics and Mechanism. *Chem. Eng. J.* **2018**, *338*, 323–332. [CrossRef]